Simulation and Optimization of Fracture Healing

D. Nolte[b,c], K. Urban[b,c], F. Niemeyer[a,c], L. Claes[a,c], U. Simon[a,c]

[a] Institute of Orthopaedic Research and Biomechanics, Ulm University, Germany
[b] Insitute for Numerical Mathematics, Ulm University, Germany
[c] Scientific Computing Center Ulm (UZWR), Ulm University, Germany

Abstract

The objective of this paper is to present an optimization algorithm for the optimization of the axial stiffness of a fixator used in fracture healing. To this end, numerical simulations of fracture healing with 2D and 3D models are used. The simulation is extended by a tool to observe the bridging of two bone fragments, called bridge detector. Using this bridge detector, the optimization criterion of shortest healing time can be defined and optimal fixator configurations can be estimated using approximations of the healing time function. As an outlook to further research, an analytical model of a 1D healing simulation and an algorithm to calculate an optimal control for the fixation is presented.

1 Numerical Simulation

The problem of fracture healing is a field of great interest for orthopaedic research. Up to now, it is not fully understood under which conditions a healing of fractures can be guaranteed and how this process finishes as fast as possible. To avoid animal experiments in this research, numerical simulations are developed. In this work, we restrict our attention to numerical simulations presented in [19] as 2D model and in [17, 18] as 3D model.

1.1 Medical Problem

The considered kind of fracture healing takes place in long bones with a fracture gap between the fracture parts. Around this fracture gap a callus builds up to increase the diameter. This callus is initially composed of soft tissues such as granulation tissue and connective tissue. These soft tissues are replaced by cartilage due to chondrogenesis, which might be replaced to woven bone (enchondral ossification) or connective tissue can directly be replaced by woven bone (intramenbranous ossification). Also the process of destruction of cartilage and woven bone back to connective tissue is modeled in the simulation. These different processes of tissue differentiation are influenced by local stimuli such as the vascularity of the tissue, mechanical strains, the tissue concentrations in the surrounding and others. After the healing process is finished and there is a bony connection of the fragments, the woven bone is displaced by laminar bone and the callus is decomposed in the remodeling process, such that finally the bone gets its initial shape.

1.2 Numerical Model

Several different models for the fracture healing have been developed. The differences of these models are in the influence of the mechanical and biological influences. For the local mechanical signals influencing the tissue differentiation, strain invariants ([5, 8, 11]) or the strain energy density ([2, 3]) is used.

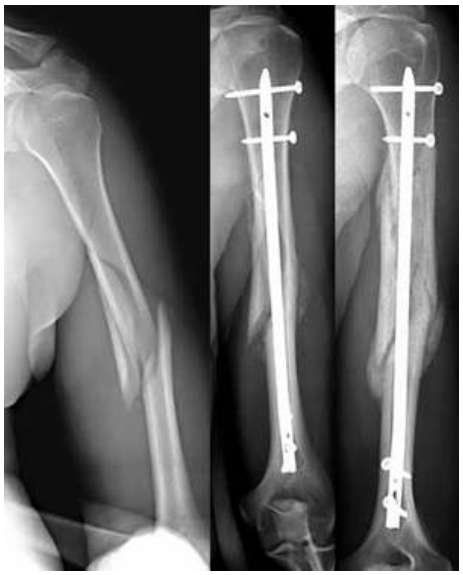

Figure 1: X-ray images of a humerus fracture, fixation using an intramedular nail and the callus build arround the fracture gap during the healing process.

Other healing simulations use a poroelastic mechanical model and use also the fluid velocity ([12, 13]) or the fluid shear stress ([15]) in addition. Also biological factors like local concentrations of growth factors ([4, 5]) or mesenchymal stem cells ([12, 13]) are considered.

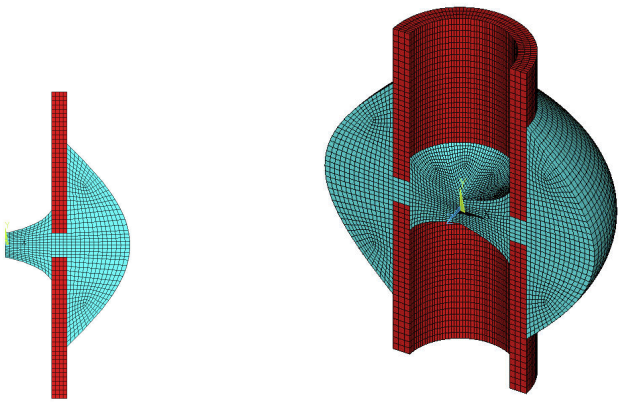

Figure 2: Finite element grid of the 2D and 3D callus model with the cortical bone (red) and the soft tissue (blue).

In the considered numerical simulation of the healing process ([17, 18, 19]), only the processes after building the callus with connective tissue and before the remodeling process starts is simulated. For the simulation of the fracture healing process, the geometry of the callus is modeled and is assumed to be constant over time. In the simplest case, the geometry is assumed to be axisymmetric. Thus, the callus can also be build as a 2D axisymmetric model in the case of an outer mechanical stimulus in axial direction of the bone. The geometry is subdivided into quadrilaterals in the 2D, axisymmetric case, or into hexahedrons in the 3D case. For each element in the grid, the percentage of the three types of tissues and the percentage of the vascularity is modeled under the assumption, that there are no holes in the callus, i.e.,

the concentrations of the three different tissues sum up to one.

The time of the healing simulation is discretized equidistantly in one day time periods. For this time discretization, the changes of tissue and vascularity are modeled by using a fuzzy logic controller. This method for simulating tissue transformations was first introduced in [2] and was extended by the influence of the vascularity in [19]. The input of this fuzzy logic controller are the concentrations of tissue, the rate of vascularization and the maximal values for bone and vascularity in the neighboring elements and the distortional and dilatational strain under a given load. In the simplest case, we only consider axial loads with a constant force over the whole time period. The strains are calculated by using the finite element method for a linear elastic, isotropic material model. For this FEM analysis, the same grid as used for the discretization of the tissue concentrations and the vascularity is used. The material properties for the mechanical model, i.e., the Young's modulus and the Poisson's ratio, are estimated by a rule of mixture. The Poisson's ratio is estimated as weighed sum of the tissue concentrations in an element of the grid, i.e.,

$$\nu = \nu_{\text{bone}} c_{\text{bone}} + \nu_{\text{cart}} c_{\text{cart}} + \nu_{\text{conn}}(1 - c_{\text{bone}} - c_{\text{cart}}),$$

where $\nu_{\text{bone}}, \nu_{\text{cart}}$ and ν_{conn} are the assumed Poisson's ratios for pure tissues of woven bone, cartilage and connective tissue, respectively, and c_{bone} and c_{cart} are the bone and cartilage concentrations of an element. The modulus in an element is estimated by

$$\begin{aligned} E = \quad & E_{\text{conn}} + (E_{\text{bone}} - E_{\text{conn}}) c_{\text{bone}}^3 \\ & + (E_{\text{cart}} - E_{\text{conn}})(c_{\text{cart}}^3 + 3c_{\text{cart}}^2 c_{\text{bone}} + 3c_{\text{cart}} c_{\text{bone}}^2), \end{aligned} \tag{1}$$

where $E_{\text{bone}}, E_{\text{cart}}$ and E_{conn} are the assumed modulus of woven bone, cartilage and connective tissue, respectively. The idea of the equation is, that the E-modulus of two tissues with different moduli raises from the lower to the higher with the third power of the concentration of the tissue with the higher modulus (cp.[7]). This is just a small change of the introduced estimation of the modulus in [19] to fix some unexpected effects of the former equation.

2 Bridging Criterion

To define a healing time for the numerical simulation, the first bridging of the fracture parts, i.e., the duration until a path of neighboring elements with a minimal bone concentration connecting two elements from the different parts of the bone exists, is observed. For the minimal bone concentration an arbitrary value of 88.9% is used. The procedure to observe the bridging of the bone parts is presented in [14], the so called bridge detector.

For the bridge detector, the grid is interpreted as a graph, where each element is a node in the graph. Two nodes are linked by an edge if they are defined as neighbors, that is two elements have a common face in the grid. For this graph an A^*-algorithm is used to search a path between two elements, each from one part of the corticalis. The bridge detector returns the number of used iterations, i.e.,the time in days for a one day step size. Additionally, an approximation of the time the bridging happens before the last time step is returned.

3 Optimization

The healing simulation with bridge detector can be used to estimate an optimal fixation in terms of a minimal healing time. For the optimization algorithm we have to notice that we do not have any information about the derivative of the healing time function with respect to the fixation stiffness:

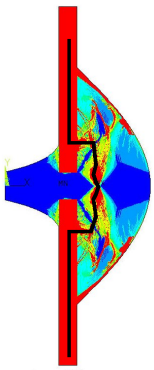

Figure 3: Bridging of fragments in the numerical simualtion. Presented is an image of the bone concentrations from low concentrations (blue) to high concentrations (red) and a path of high bone concentrations between the fragments.

The analytical formulation of the fuzzy controller is too complex to estimate any derivatives. Currently, it is not possible to determine derivatives by automatic differentiation because the source code of the finite element simulation of the model, which is implemented in ANSYS, is not available. The approximation of the derivatives by using finite differences is also not feasible because for higher stiffnesses the function values increase very slowly and have perturbations in the magnitude of the increase of the function (cp. Figure 4). Thus, an approximation with cubic splines is used to get a smooth function which can be minimized. This type of approximation is used to fit the function values, which have been estimated on an equidistant grid.

For the minimization of the approximation almost any optimization algorithm is suitable because the cost of the optimization of a B-spline is marginal compared to the cost of estimating the grid points of the healing time function. The used optimization method of the NAG C library (e04abc) is based upon the optimization of real-valued functions by the quadratic-interpolation function of Gill and Murray, which searches the minimum of the function by minimization of quadratic interpolation and reducing the starting interval of the algorithm.

This optimization algorithm is used with different starting points, e.g., for all calculated grid points, to estimate all local minima. The global minimum can then be taken from the set of minima for all chosen starting points.

3.1 Results

The presented results are estimated for an average grid-size for the discretization in space. The minima for different numbers of spline intervals from 2 to 19 vary from about $1500\frac{N}{mm}$ to $3000\frac{N}{mm}$ for the axial stiffness of the fixation, where the approximated function values are in most cases much better than all estimated function values of the healing time function. The estimated range of the optimal stiffness for the fixation fits to the impression one gets from the function values of the healing time function. As can be seen from the spline approximations and the wide range of optimal values for the optimal fixation, the presented method is not very reliable. Another drawback is, that the function values of the healing time function are not as smooth as expected.

The stiffness range called to be optimal lies in between the axial stiffness of known fixations. Unilateral external fixators are softer ($\approx 500\frac{N}{mm}$), intramedular nails are stiffer ($\approx 3000\frac{N}{mm}$) than the predicted optimum.

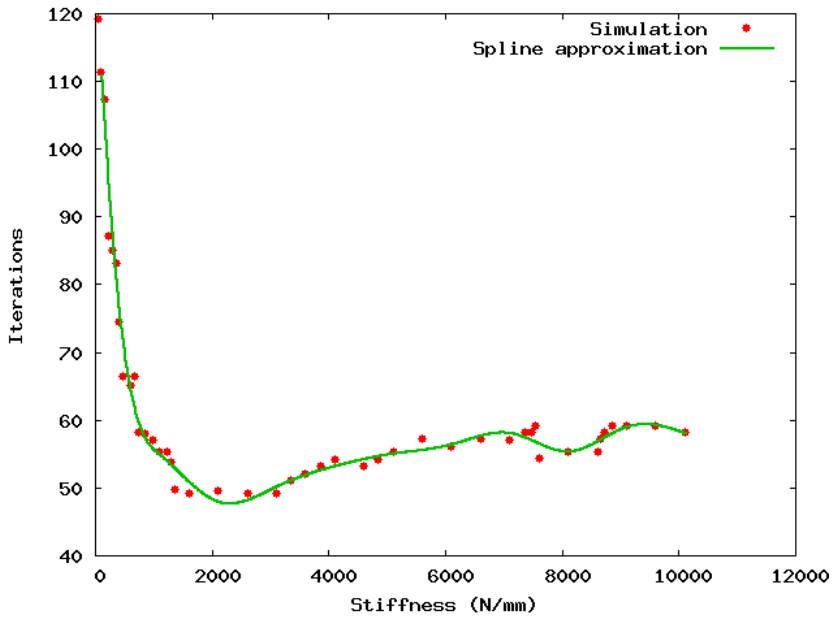

Figure 4: Healing times of the 2D healing simulation with average grid size of $0.2mm$ and a spline approximation of the healing-time function with 10 spline nodes.

4 1D Simulation and Optimal Control

As a simplification of the fracture healing simulation, a 1D model is build. In this model, the callus of length ℓ is modeled by the area of the profile $A(x)$, $x \in [0, \ell]$, along the axis of the callus. As a simplification, the symmetry of the callus can be used. Thus, only one half of the callus has to be modeled. The concentrations of bone, cartilage and vascularity are described by the vector

$$\boldsymbol{c}(t,x) = \left(c_{\text{bone}}, c_{\text{cart}}, c_{\text{vasc}}\right)^T(t,x)$$

at time t in location x as in the 2D and 3D model.

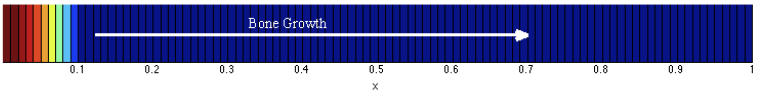

Figure 5: 1D model of the bone concentration growth with initially high bone concentration (red) on the left and low bone concentration (blue) on the right.

For the tissue differentiation, we use the fuzzy controller of the 2D and 3D model. The only difference to the input variables is that there is only one strain variable as input. To use the fuzzy controller, we fix a value for the dilatational strain and use the distortional strain as a variable.

The strain is estimated using a model of a system of two parallel springs with stiffnesses k_{cal} and k_{fix} for the callus and the fixation. Thus, the force F of the load to the system splits into the two forces to the callus and fixation, i.e.

$$F = F_{\text{cal}} + F_{\text{fix}}, \tag{2}$$

and similar the stiffnesses

$$k = k_{\text{cal}} + k_{\text{fix}}. \tag{3}$$

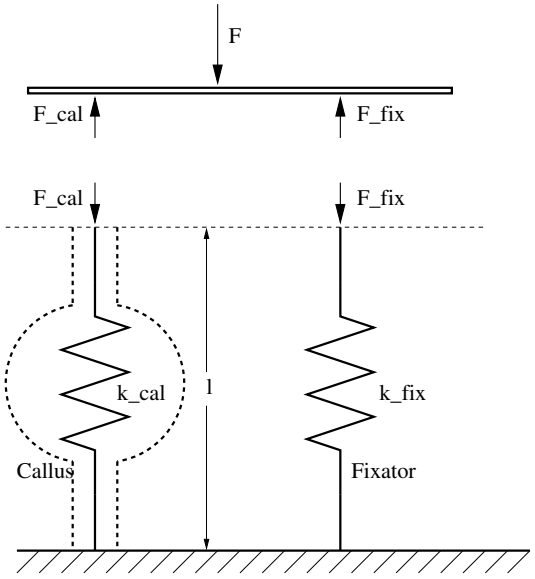

Figure 6: Mechanical Model of callus and fixator in 1D.

From the definition of a spring stiffness we have

$$k_{\text{fix}} = \frac{F_{\text{fix}}}{d\ell}, \tag{4}$$

where $d\ell$ is the difference of the length of the spring of unloaded and loaded case. The linear elastic mechanical law for the callus is given by

$$\begin{aligned} \varepsilon &= u', && (5)\\ \sigma &= E\,\varepsilon, && (6)\\ (A\,\sigma)' &= 0, && (7) \end{aligned}$$

with the boundary conditions

$$\begin{aligned} A(\ell)\,\sigma(\ell) &= F_{\text{cal}}, && (8)\\ u(0) &= 0. && (9) \end{aligned}$$

Here, u is the displacement, σ is the stress, ε the strain and E is the Young's modulus.

As in the 2D and 3D model, the modulus is a function of the tissue concentration, i.e., $E = E(\boldsymbol{c}(t,x))$, and also the stress, strain and displacement: $\sigma = \sigma(x, \boldsymbol{c}(t,\cdot))$, $\varepsilon = \varepsilon(x, \boldsymbol{c}(t,\cdot))$ and $u = u(x, \boldsymbol{c}(t,\cdot))$. From (7) and (8) one gets that

$$A(x)\,\sigma(x, c(t,\cdot)) = F_{\text{cal}} \quad \forall x \in [0,\ell], \tag{10}$$

and the strain can be calculated by

$$\varepsilon = \frac{F_{\text{cal}}}{A\,E}. \tag{11}$$

The change of the length of the callus can be written as

$$d\ell = \int_0^\ell u'\,dx = \int_0^\ell \varepsilon\,dx = F_{\text{cal}} \int_0^\ell \frac{1}{A\,E}\,dx. \tag{12}$$

Thus, the callus stiffness can be calculated by

$$k_{\text{cal}} = \left(\int_0^\ell \frac{1}{A\,E}\,dx \right)^{-1}. \tag{13}$$

The change of the lenght in terms of the stiffness of the whole system is

$$d\ell = \frac{F}{k} = \frac{F}{k_{\text{fix}} + k_{\text{cal}}}, \tag{14}$$

and the force to the callus is

$$F_{\text{cal}} = k_{\text{cal}}\, d\ell = \frac{F}{k_{\text{fix}} + k_{\text{cal}}} k_{\text{cal}}, \tag{15}$$

the strain can be calculated by using (11), (13), and (15) as

$$\varepsilon = \frac{F k_{\text{cal}}}{A\, E\, (k_{\text{fix}} + k_{\text{cal}})}. \tag{16}$$

The healing of the fracture can be observed directly in the 1D model by comparing the bone concentration at the endpoint of the model to a lower bound c_∞. This can be done without the bridge detector. Another advantage is that there is no choice for the direction of the bone growth. The bone will grow towards the middle of the callus. Hence, to observe a minimal healing time, the bone growth has to be maximized. Therefore, the fuzzy logic is optimized to gain maximal bone growth.

To obtain the optimal values of the fuzzy controller for bone growth and also cartilage growth and maximal growth of vascularity, the fuzzy controller is optimized using a Monte Carlo method. Therefore, the fuzzy logic controller is evaluated at a random set of parameters (between 10000 and 50000 parameterss). From these function values, the maximal values for each component of the output parameter is chosen and the set of optimal input parameters is estimated. Because the fuzzy controller is a piecewise linear, continuous function which is constant in most parts of the domain, the resulting sets of optimal control parameters describe small, seven-dimensional intervals of the domain. From the results of the optimization, it can be seen that optimal bone growth only depends on five input parameters, i.e., the bone concentration in place and in the neighborhood, the vascularity and the strains. In the 1D case, the dilatational strain is chosen fixed to gain optimal bone growth. Thus, the fuzzy controller depends only on four parameters.

To obtain an algorithm to estimate an optimal healing, we rewrite (16) as

$$k_{\text{fix}} = \frac{F\, k_{\text{cal}}}{\varepsilon\, A\, E} - k_{\text{cal}} \tag{17}$$

Using an optimal value for the strain, an optimal stiffness of the fixator can be calculated.

To formulate a numerical algorithm, a discretization in time and space is used, especially the discretization of time is used in the following algorithm:

Given an inital bone concentration $\boldsymbol{c}^0(x)$.

1. Find $I \subset [0, \ell]$, i.e., a set of grid points in the discretization, where an optimal bone growth can be observed, i.e., where the concentrations for bone and vascularity are optimal for bone growth and $\boldsymbol{c}(t, x) \leq c_\infty$.
2. Estimate a stiffness of the fixator by (17), such that the bone growth is optimal in the chosen selected interval.
3. If $c(t, \ell) \geq c_\infty$, stop. Otherwise update the tissue by calculating the changes with the fuzzy logic controller for the grid points in space and continue with 1.

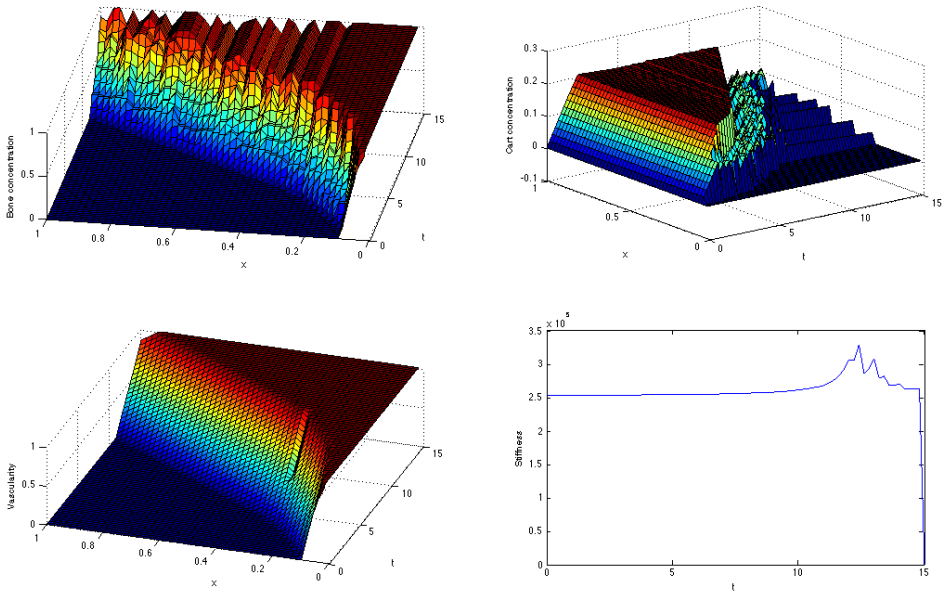

Figure 7: Optimal control for the 1D healing model: shown are the bone concentration over time and space (upper left), cartilage concentration over time and space (upper right), vascularity over time and space (lower left) and the estimated fixator stiffness over time (lower right).

4.1 Results

To test the presented algorithm, we choose an area function $A(x) = 1$ for $x \in [0, 1]$, and initial values for the concentrations

$$\boldsymbol{c}^0(x) = \begin{pmatrix} c^0_{\text{bone}}(x) \\ c^0_{\text{cart}}(x) \\ c^0_{\text{vasc}}(x) \end{pmatrix} = \begin{pmatrix} \cos\left(\frac{\pi x}{0.2}\right)\ \chi_{[0,0.1]}(x) \\ 0 \\ \cos\left(\frac{\pi x}{0.2}\right)\ \chi_{[0,0.1]}(x) \end{pmatrix},$$

where $\chi_A(x)$ is the characteristic function of a set A.

The results of the simulation are shown in Figure 7. It can be seen that the algorithm can compute a control for the 1D model which leads to a healing. By comparing the elapsed healing time to the optimal time which comes from the maximal bone growth from the fuzzy logic it can be seen, that the control of the stiffness is almost optimal.

5 Discussion

It has been shown that the 2D and 3D fracture healing model can be used to estimate an optimal stiffness of the fixator for the shown model. But in fact, the used optimization algorithm is not very accurate. The resulting interval of optimality is too big to predict an optimal healing for any choosen parameter in the interval. The main reason why the optimization does not allow a precise prediction of an optimal fixator is, that the healing time function with the two parts simulation and bridge detector is not as smooth as expected. The function values seem to have perturbations which may come up from the discretization of the callus and the connection of the gridsize of time and space.

To get a deeper insight to the behavior of the fuzzy logic controller, the 1D model was build. By optimization of the fuzzy controler, an algorithm could be implemented that is able to calculate an optimal control for the fixator stiffness. This 1D model is not able to predict any healing processes of real fracture. But the idea of maximization of bone growth over the interval leads to a fast and almost optimal healing. An approach to carry the idea of optimization of bone growth from the 1D model to higher dimensions is to maximize the bone growth on a predicted path inside the callus to minimize the healing time.

Another insight of the presented optimization algorithm is, that the model of fracture healing has to be improved in the future. The model is able to predict an optically good approximation of the real healing process but it has to be improved to get reliable results as prediction for an optimal healing process.

References

[1] W. Alt. *Nichtlineare Optimierung*. Vieweg, 2002.

[2] Ch. Ament and E. P. Hofer. A fuzzy logic model of fracture healing. *Journal of Biomechanics*, 33:961–968, 2000.

[3] Ch. Ament, E.P. Hofer, and L. Claes. Fuzzy logic as a method to describe tissue adaption in fracture healing. *Transaction of the 41st Annual Meeting of the Orthopaedic Research Society*, 1995.

[4] A. Bailón-Plaza and M. C. H. van der Meulen. A mathematical framework to study the effects of growth factor influences on fracture healing. *Journal of Theoretical Biology*, 2(212):191–209, June 2001.

[5] A. Bailón-Plaza and M. C. H. van der Meulen. Beneficial effects of moderate, early loading and adverse effects of delayed or excessive loading on bone healing. *Journal of Biomechanics*, 36:1069–1077, March 2003.

[6] D. P. Bertsekas. *Dynamic Programming and Optimal Control*, volume 1. Athena Scientific, 1995.

[7] D. R. Carter and W. C. Hayes. The compressive behaviour of bone as a two-phase porous structure. *The Journal of Bone and Joint Surgery*, 59-A(7):954–962, October 1977.

[8] M. Doblaré, J.M. García, and M.J. Gómez. Modelling bone tissue fracture and healing: a review. *Journal of Engineeing Fracture Mechanics*, 71:1809–1840, 2004.

[9] H. Goeldner. *Lehrbuch Höhere Festigkeitslehre Band 1*. VEB Fachbuchverlag Leipzig, 1984.

[10] H. Goeldner and F. Holzweissig. *Leitfaden der Technischen Mechanik*. VEB Fachbuchverlag Leipzig, 1980.

[11] M.J. Gomez-Benito, J.M. Garcia-Aznar, J.H. Kuiper, and M. Doblaré. Influence of fracture gap size on the pattern of long bone healing: a computational study influence of fracture gap size on the pattern of long bone healing: a computational study influence of fracture gap size on the pattern of long bone healing: a computational study. *Journal of Theoretical Biology*, 2005.

[12] D. Lacroix and P. Prendergast. A mechano-regulation model for tissue differentiation during fracture healing: analsysis of gap size and loading. *Journal of Biomechanics*, 35(9):1163, 2002.

[13] D. Lacroix and P. Prendergast. Three-dimensional simulation of fracture repair in the human tibia. *Computer Methods in Biomechanics and Biomedical Engineering*, 5(5):369–376, 2002.

[14] F. Niemeyer. Entwicklung und Programmierung von Algorithmen zur klinisch relevanten Auswertung zeitabhängiger, dreidimensionaler Daten simulierter Frakturheilungsprozesse. Master's thesis, Universität Ulm, 2007.

[15] Royal Academy of Medicine in Ireland. *Computational Simulation of Fracture Callus Fromation and Stiffness Restauration*. Proc. of Proceedings of the 12th Conference of the European So-, 2000.

[16] H. R. Schwarz. *Numerische Mathematik*. Teubner, 1997.

[17] U. Simon, P. Augat, and L. Claes. 3d fracture healing model can help to explain delayed healing with interfragmentary shear movement compared to axial movement. In *Proceedings of the 6th International Symposium on Computer Methods in Biomechanics and Biomechanical Engineering*, 2004.

[18] U. Simon, P. Augat, and L. Claes. Delayed healing of fractures with interfragmentary shear movement can be explained using a 3d computer model. In *Proceedings of 13th Conference of the European Society of Biomechanics*, 2004.

[19] U. Simon, P. Augat, M. Utz, and L. Claes. A numerical model of the fracture healing process that describes tissue development and revascularization. In *Computer Methods in Biomechanics and Biomedical Engineering, In review process*, 2005.

[20] J. Stoer. *Numerische Mathematik 1*. Springer, 1999.